Shahrood University of Technology
Iranian Society of Mining Engineering (IRSME)
Journal of Mining and Environment (JME)
journal homepage: www.jme.shahroodut.ac.ir
THOMSON REUTERS

Interaction between Tunnel and Surface Foundation using PFC2D

Vahab Sarfarazi[1*], Kaveh Asgari[2] and Shadman Mohamadi Bolban Abad[1]

1- Department of Mining Engineering, Hamedan University of Technology, Hamedan, Iran
2- Department of Mining Engineering, Shahid Bahonar University of Kerman, Kerman, Iran

Article Info

Received 17 May 2021
Received in Revised form 11 June 2021
Accepted 17 June 2021
Published online 17 June 2021

DOI:10.22044/jme.2021.10846.2057

Keywords

Tunnel
Foundation
PFC
Settlement
Collapse zone

Abstract

In this work, we investigate the interaction between tunnel and surface foundation in two dimensions by the particle flow code. At the first stage, the PFC calibration is conducted using the experimental test results rendered by a biaxial test. Then the simulation of a biaxial test is performed by confining a rectangular sample inside four walls. The walls are located at the top and bottom simulated loading plates and the adjacent walls are located at the left and right simulated sample side confinement. The velocities of the top and bottom walls are determined, and they are used for loading the sample in a strain-controlled mode. The respond of the material is evaluated by following the diverse stress and strain quantities. The axial deviatoric stress versus the axial strain for biaxial test on the bonded granular material is drawn, and then the Mohr's circle is drawn in order to reach the failure envelope of laboratory. Secondly, a rectangular model with dimensions of 10 m × 10 m containing a central tunnel and a surface foundation is built. The tunnel is situated in sixteen different positions below the foundation. The foundation moves downward with a velocity of 0.016 mm/s. The results obtained show the position of the tunnel controlling the failure volume. Also the vertical displacement at the roof of the tunnel decreases by increasing the vertical spacing between tunnel and foundation. The settlement beneath the foundation increases by reducing the vertical spacing between the tunnel and the foundation. The settlement beneath the foundation decreases by augmenting the horizontal spacing between the tunnel and the foundation.

1. Introduction

Due to the increasing population in the urban areas, there is an essential requirement for the development of infrastructures, and this demand has also led to extending construction of a new metro system and tunnels in the cities of Iran. Through tunneling in urban areas, usually a tunnel should build a pile-supported building or bridge. In these kind of circumstances, the foundations of the adjacent pile bridges or buildings because of movements of ground due to the tunneling may tolerate negative effects and result in some foundational systems experincing more displacement. Furthermore, it leads to an increase in the stresses to the others (Lee [1]). General processes of tunneling in the urban areas usually occur in unappropriate ground circumstances, so in the condition of associating the existing surface and sub-surface structures with the tunneling process, the impact of the process on the existing structures shoud be evaluated during the design and construction levels. Movement of ground caused by single tunneling has been widely studied by several ways such as field observation (e.g. [2-4]), analytical method (e.g. [5, 6]), numerical modelling (e.g. [7-20]), and physical modelling (e.g. [21, 22] Mair, 1979; Taylor, 1984). Furthermore, investigation of the ground movements caused by multiple tunneling has been carried out. Some researchers have shown that the surface settlement troughs due to twin tunnels have different shapes (e.g. [23-24]). In the case of studying the movement associated with multiple tunneling, due to the lack of field data, the investigators have generally used numerical

Corresponding author: vahab.sarfarazi@gmail.com (V. Sarfarazi).

modelling (e.g. [25-36]) and physical modelling (e.g. [37-39]). It is clear that both the numerical and physical modellings give a valuable insight, although due to the inherent uncertainties in tunnel engineering, the settlement quantities determined by these kinds of investigations can rarely represent the actual quantities found in a real condition. Yoo [40] has announced that the recent application of the New Australian Tunneling Method (NATM) within the urban areas due to augmenting these kinds of complicated ground circumstances has increased, while the principles of NATM, created by Rabcewicz [41] and Muller [42], were extended for tunneling under competent ground situations. During the application of NATM below an existing structure or bridge, determining the results and the impacts on the existing structures are essential. There are several investigations in the field of tunneling below the existing pile (e.g. Vermeer [43]; Chen [44]; Mrouhe [45]; Lee [46]; Cheng [47]; Yoo [48]; Lin [49]; Lin [50]). These research works have generally indicated the vital governing mechanism of the impact of tunneling on the area of the existing pile, except an investigation by on Yoo [48], most of them have concentrated on the idealized tunneling conditions or simplified plane strain assessments. These investigations indicate the results of a 2D Particle Flow Code (PFC) numerical examination in conventional tunneling below an existing surface foundation. In fact, the effect of the distance between tunnel and foundation on the failure zone have been investgated.

2. Particle Flow Code (PFC)

One of the models that can be used in order to assess the model particles cyclically is that the PFC2D model could be a set of separate circular particles, and uses the express time-step circulation rule (Itasca [51]; Potyondy and Cundall [52]; Designer [53-54]). The contact force between the particles is predicated on the law of force–displacement, and therefore, the particle motions are in step with the Newton's second law. As a discrete element model (DEM), the ‘‘contact bond model’’ and ‘‘parallel bond model’’ are two main forms of the bond particle model. In the first model, the particles are attached together with an extent of glue, and torque cannot be transferred by contacts, whereas in the latter model, the particles are attached by a surface layer of glue. Besides, the rotation of particles induces a torque that can be tolerated by contacts. Therefore, the parallel bond model can introduce a cement-like material like rock. We used the model of linear contact in this investigation that established an elastic relationship between the relative displacements and the contact forces of particles. In the case of using the routines provided (Itasca [49]), in order to produce a parallel-bonded particle model for PFC2D, some properties must be introduced: stiffness ratio kn over ks, modulus of ball-to-ball contact, coefficient of ball friction, standard deviation ratio to bond strength mean both in the shear and normal directions, parallel normal bond strength, parallel-bond radius multiplier, minimum ball radius, parallel-bond modulus, parallel shear bond strength, and parallel-bond stiffness ratio, ratio of the standard deviation to the mean of bond strength both in the normal and shear directions. For establishment of the micro-properties used for assembly of the particles, it is essential to determine a calibration approach. For a direct representation of the properties of the particle contact and bonding, the laboratory model samples are not suitable. In the nature, the characteristics of the materials specified by the laboratory experiments are macro-mechanical, and this is due to the continuum behavior. Due to the aforementioned contents, an inverse modelling approach was applied in order to specify the suitable micro-mechanical characteristics of the numerical models from the macro-mechanical characteristics specified in the laboratory experiments. One of the procedures that is being applied to correlate these two sets of substance characteristics is the trial-and-error approach (Itasca [49]). This method assumes the micro-mechanical characteristic values, and provides a comparison between the strength and deformation properties of the numerical models and laboratory experiments. Finally, the simulation value of the micro-mechanical of the macroscopic response having the closest value to the laboratory tests were chosen for evaluating the ground settlement.

2.1. Numerical model preparation and calibration

In order to calibrate the compressive strength and young modulus of the sample in the PFC2D model, the uniaxial compression test was used. The standard procedure of production of a PFC2D assembly to determine a test model includes 4 steps: (a) generating and compression of particles, (b) installation of isotropic stress, (c) buoyant particle deletion, and (d) installation of bond. In PFC2D, a biaxial test is simulated by confining a

rectangular specimen (including a packed particle assembly) inside four walls (Figure 1). The specimen was made of 12,615 particles. The top and bottom walls and the left and right walls simulate the loading plates and the confinement experienced by the specimen sides, respectively. The specimen is loaded in a strain-controlled mode by determining the velocities of the upper and lower walls (0.016 m/s). The stresses and strains tolerated by the specimen are specified in a macro-mode by summing the forces acting upon and the relative spacing between the appropriate walls. The substance response is evaluated by following the diverse stress and strain quantities. The axial deviatoric stress versus the axial strain for the biaxial test on the bonded granular material was drawn, and then the Mohr's circle was drawn to reach the failure envelope of laboratory. Table 1 indicates the characteristics of the alluvial soil of the city of Tehran used in this investigation [17]. The determined micro-parameters (getting from calibration) are listed in Table 2 based on the strength and stiffness criteria.

Table 1. Characteristics of the alluvial soil of the city of Tehran.

γ_{dry} (KN/m^3)	E (Kg/cm^2)	ν	C(Kg/cm^2)	φ (°)
19	750	0.35	0.3	34

Table 2. Determined micro-parameters in PFC2D (getting from calibration).

Factor	Value	Factor	Value
Type of particle	Disc	Parallel-bond radius multiplier	1
Density (kg/m^3)	3000	Young's modulus of parallel bond (GPa)	4
Minimum radius (mm)	0.27	Parallel bond stiffness ratio	1.7
Size ratio	1.56	Particle friction coefficient	0.4
Porosity ratio	0.08	Contact bond normal strength, mean (MPa)	0.002
Friction coefficient	0.5	Contact bond normal strength, SD (MPa)	0.0004
Contact Young's modulus	4	Contact bond shear strength, mean (MPa)	0.002
Stiffness ratio	2	Contact bond shear strength, SD (MPa)	0.0004

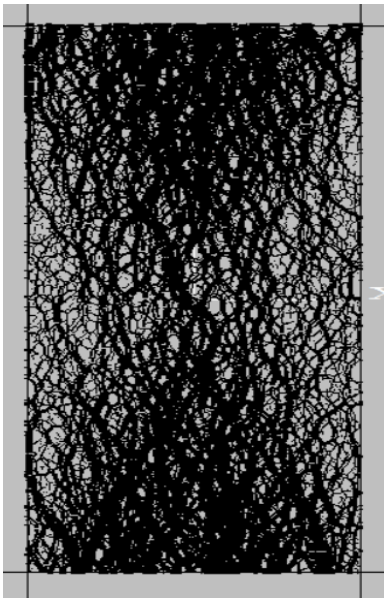

Figure 1. Contact force in the numerical model.

2.2 Preparation of model using PFC

After calibrating PFC2D, a rectangular model including a surface foundation and a tunnel was built. The dimensions of the rectangular model were 100 m × 100 m. The tunnel diameter was 10 m. The center of the tunnel was situated in 20 different positions below the surface foundation (Figures 2-5). "b" in Figure 2a changes from 15 m to 55 m with increasing 10 m, while "a" in Figure 3a changes from 0 to 30 m with increasing 10 m. For building up the rectangular sample, 18,179 disks with a minimum radius of 0.27 cm were provided. The confining pressures on the rectangular models are 0.01 MPa. The foundation moves downward with a velocity of 0.016 mm/s. For measurement of the vertical displacement, two measuring circles with a diameter of 2 m were chosen beneath the foundation and at the tunnel roof. The average vertical displacement of the discs happening in these circles was determined as a ground settlement (Figure 2a).

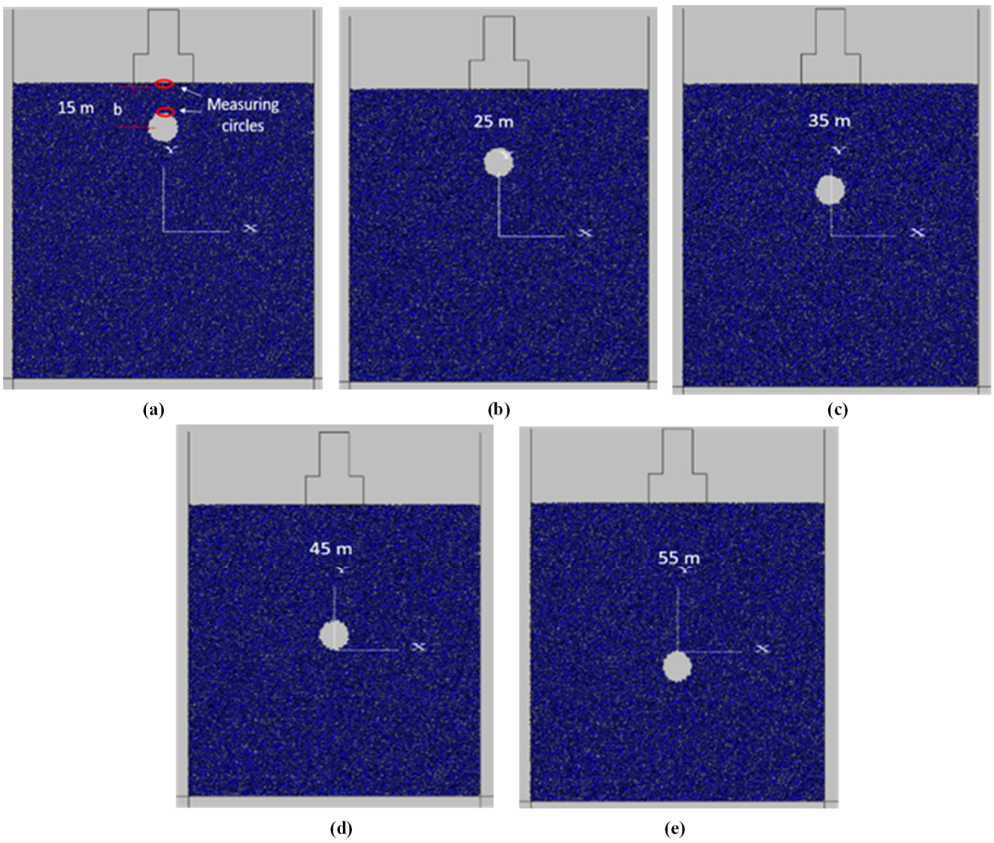

Figure 2. Tunnel was situated below the surface foundation at a vertical distance of a) 15 m, b) 25 m, c) 35 m, d) 45 m, and d) 55 m; the horizontal distance between the tunnel center and the foundation was 0 m.

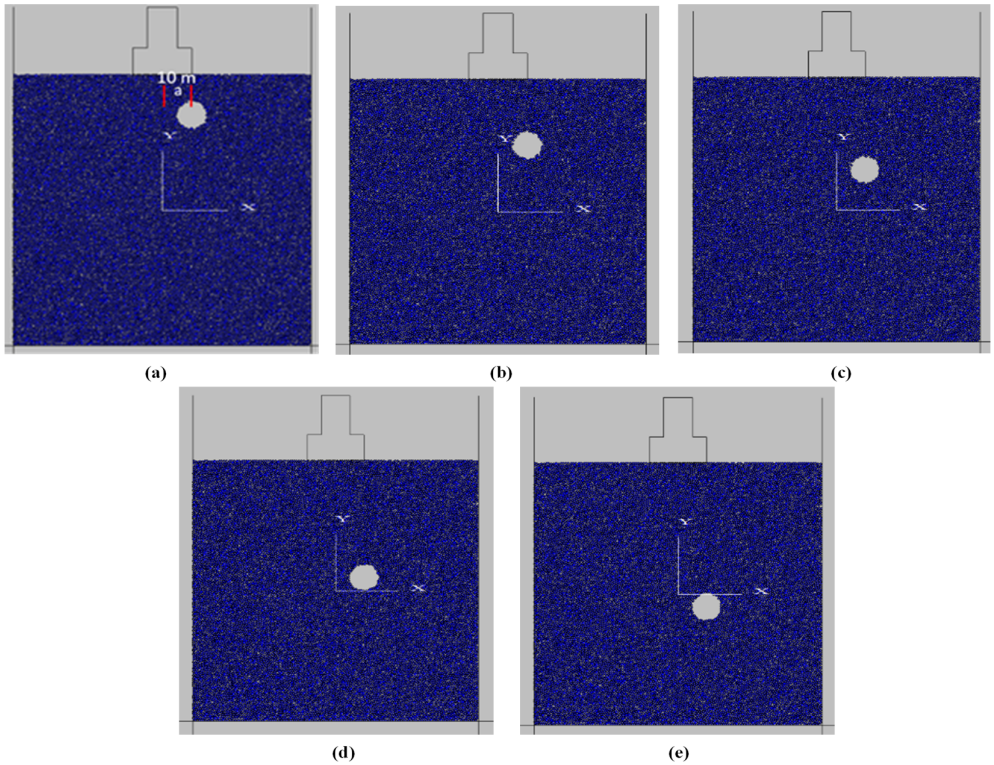

Figure 3. Tunnel was situated below the surface foundation at a vertical distance of a) 15 m, b) 25 m, c) 35 m, d) 45 m, and d) 55 m; the horizontal distance between the tunnel center and the foundation was 10 m.

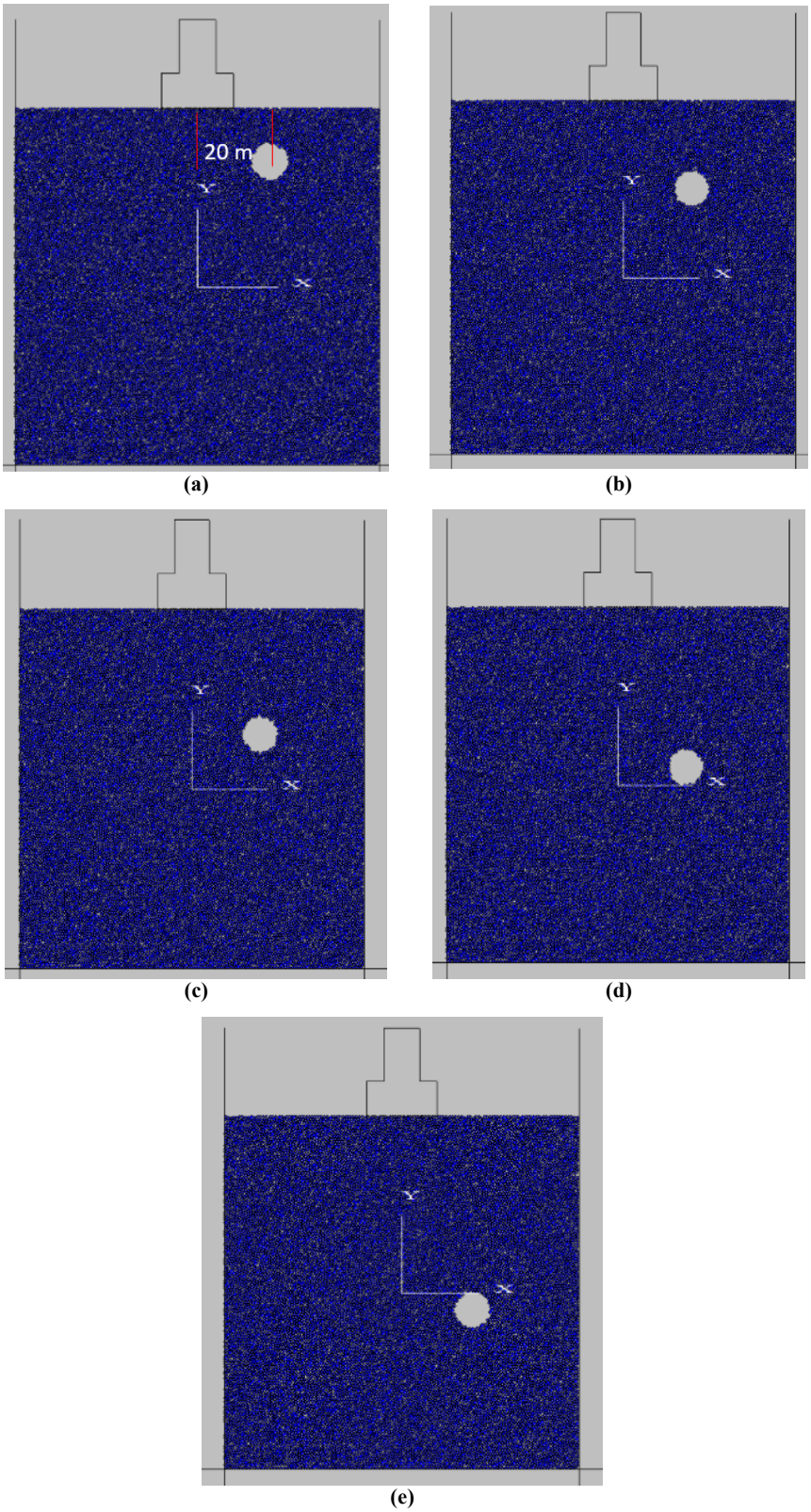

Figure 4. Tunnel was situated below the surface foundation at a vertical distance of a) 15 m, b) 25 m, c) 35 m, d) 45 m, and d) 55 m; the horizontal distance between the tunnel center and the foundation was 20 m.

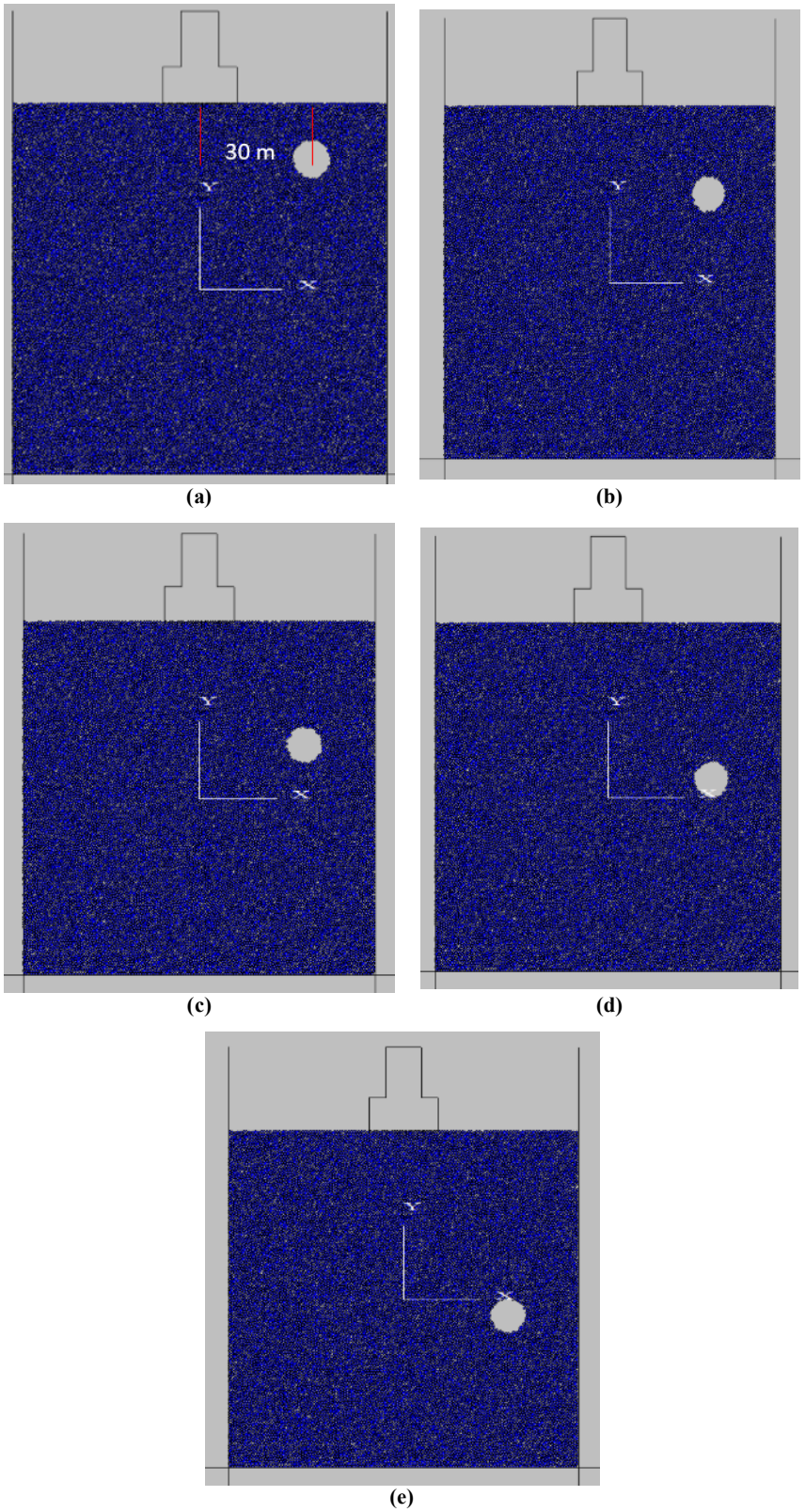

Figure 5. Tunnel was situated below the surface foundation at a vertical distance of a) 15 m, b) 25 m, c) 35 m, d) 45 m, and d) 55 m; the horizontal distance between the tunnel center and the foundation was 30 m.

3. Numerical outputs

3.1. Failure behavior of numerical models

a) When horizontal distance between tunnel and foundation is equal to 0 m:

When the vertical spacing between the tunnel center and the foundation is equal to 15 m (Figure 6), a wedge of particle colapcse occurs inside the tunnel. By augmenting the distance between the tunnel center and the foundation, the size of these wedges was decreased. It is to be noted that the particles of the side-wall of the tunnel move inside the tunnel.

b) When horizontal distance between tunnel and foundation is equal to 10 m:

When the vertical spacing between the tunnel center and the foundation is equal to 15 m (Figure 7), a wedge of particle colapcse inside the tunnel occurs. By augmenting the distance between the tunnel center and the foundation, the size of these wedges was decreased. It is to be noted that the particles of the left wall of the tunnel move inside the tunnel.

c) When horizontal distance between tunnel and foundation is equal to 20 m:

When the vertical spacing between the tunnel center and the foundation is equal to 15 m (Figure 8), a wedge of particles colapcse inside the tunnel. By augmenting the distance between the tunnel center and the foundation, the size of these wedges was decreased. It is to be noted that the particles of the left wall of the tunnel move inside the tunnel.

d) When horizontal distance between tunnel and foundation is equal to 30 m:

When the vertical spacing between the tunnel center and the foundation is equal to 15 m (Figure 9), a wedge of particles colapcse inside the tunnel. By augmenting the distance between the tunnel center and the foundation, the size of these wedges was decreased. It is to be noted that the particles of left wall of the tunnel move inside the tunnel.

From the above findings, it can be concluded that by augmenting the distance between the tunnel center and the foundation, the volume of the collapsed wedge decreases. Also the volume of the collapsed zone from the left side of the tunnel decreases by increasing the horizontal spacing between the tunnel and the foundation.

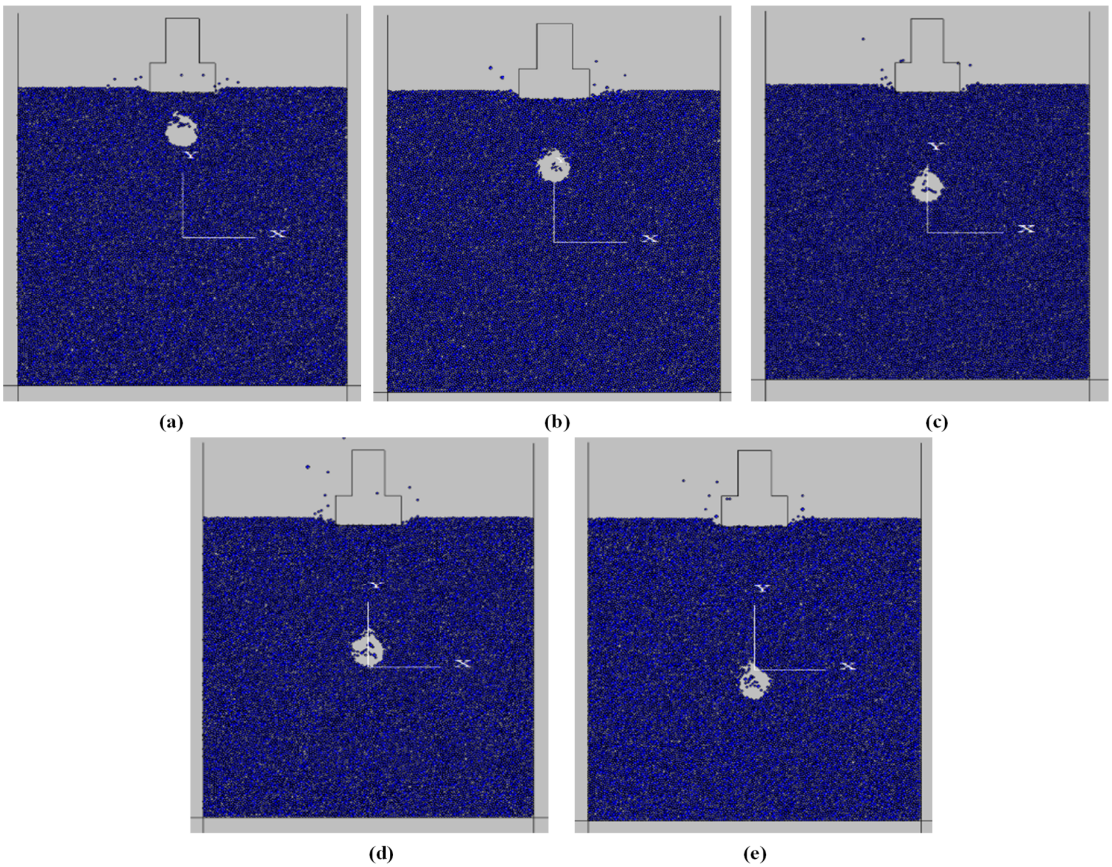

Figure 6. Failure pattern. Tunnel was situated below the surface foundation at a vertical distance of a) 15 m, b) 25 m, c) 35 m, d) 45 m, and d) 55 m; the horizontal distance between the tunnel center and the foundation was 0 m.

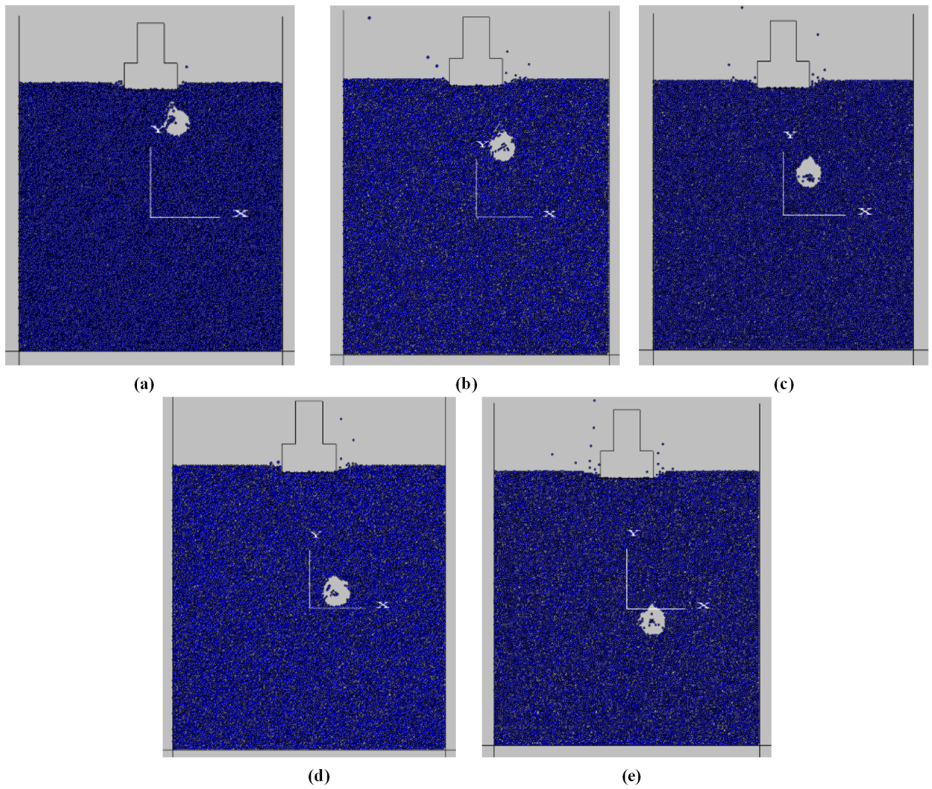

Figure 7. Failure pattern. Tunnel was situated below the surface foundation at a vertical distance of a) 15 m, b) 25 m, c) 35 m, d) 45 m, and d) 55 m; the horizontal distance between the tunnel center and the foundation was 10 m.

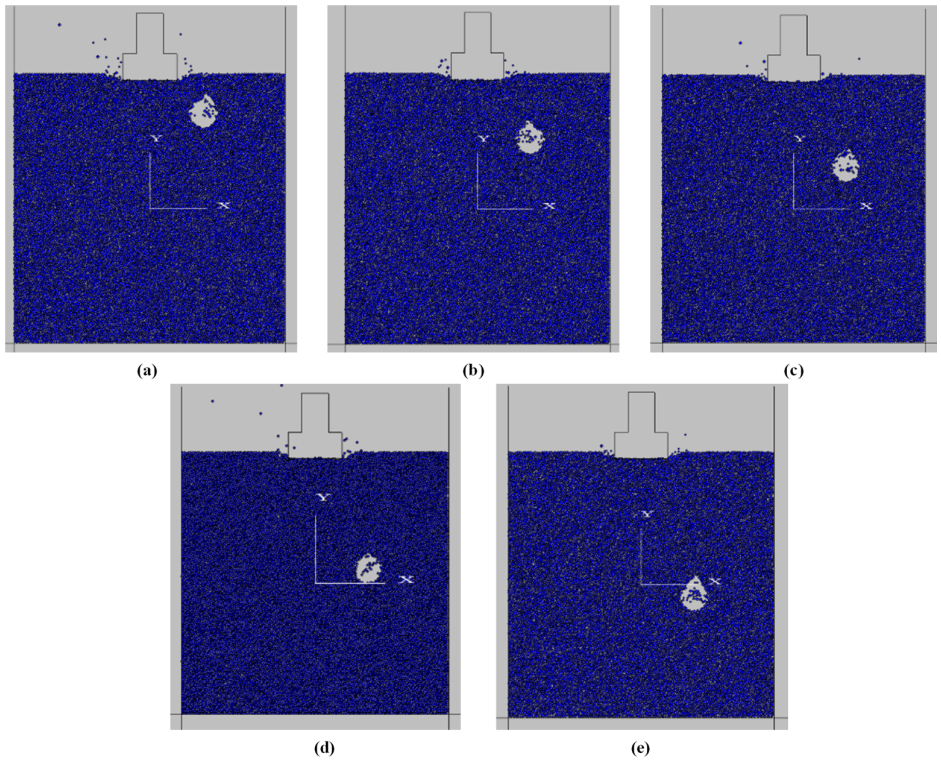

Figure 8. Failure pattern. Tunnel was situated below the surface foundation at a vertical distance of a) 15 m, b) 25 m, c) 35 m, d) 45 m, and d) 55 m; the horizontal distance between the tunnel center and the foundation was 20 m.

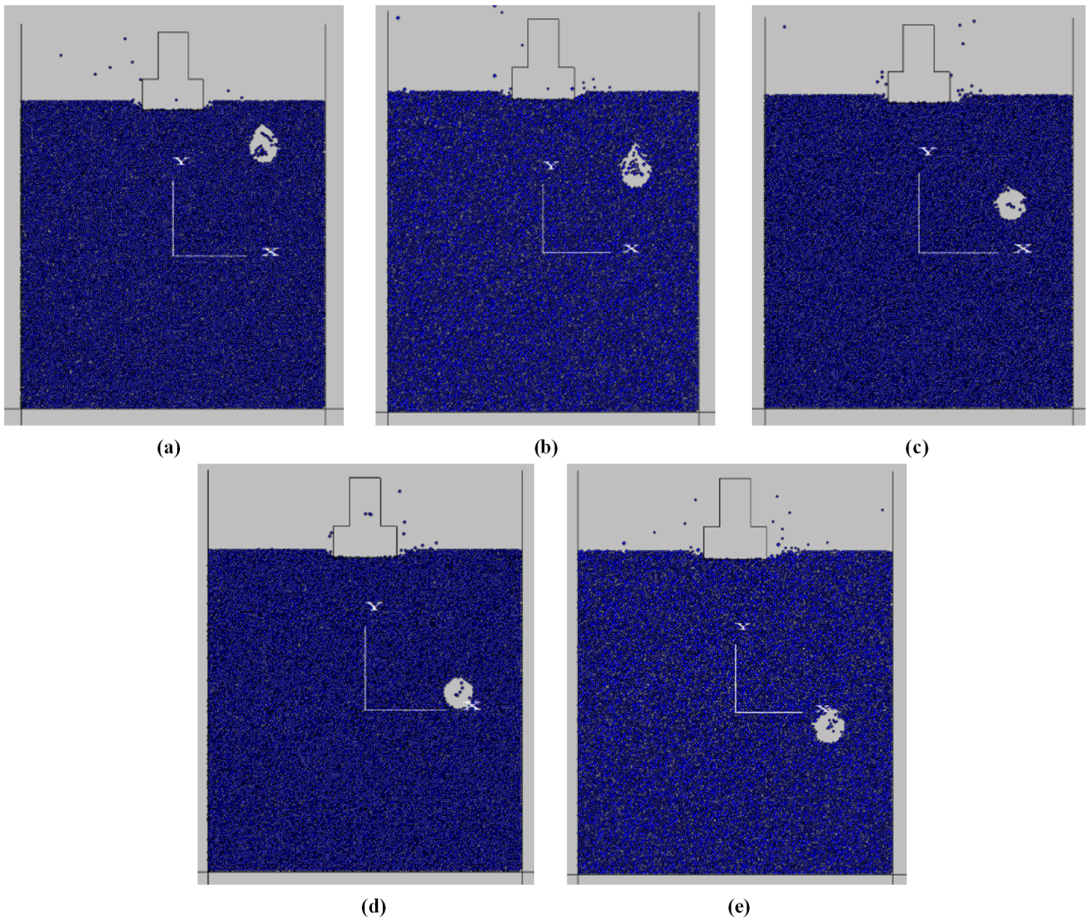

Figure 9. Failure pattern. Tunnel was situated below the surface foundation at a vertical distance of a) 15 m, b) 25 m, c) 35 m, d) 45 m, and d) 55 m; the horizontal distance between the tunnel center and the foundation was 30 m.

3.2. Tunnel position impact on ground settlement beneath foundation

Fig 10 indicates the influence of the tunnel position on the ground settlement beneath the foundation. For each configuration of the horizntal destance between the tunnel and the foundation, the ground settlement was reduced by increasing the vertical spacing between the tunnel center and the foundation. It is to be noted that the ground settlement is decresed by increasing the horizontal destance between the tunnel and the foundation.

3.3. Effect of tunnel position on vertical displacement of tunnel roof

Figure 11 indicates the impact of the tunnel position on the vertical displacement of the tunnel roof. For each configuration of the horizntal destance between the tunnel and the foundation, the vertical displacement of the tunnel roof was decreased by augmenting the vertical spacing between the tunnel center and the foundation. It is to be noted that the vertical displacement of the tunnel roof iss decreased by increasing the horizontal destance between the tunnel and the foundation.

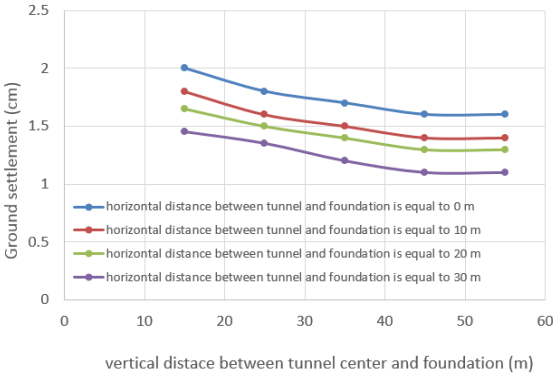

Figure 10. Tunnel position impact on ground settlement beneath foundation.

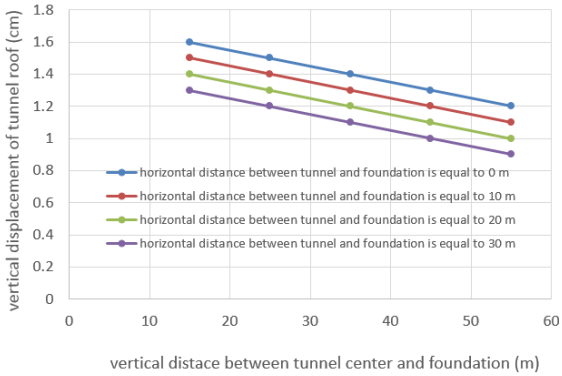

Figure 11. Tunnel position impact on vertical displacement of tunnel roof.

3.4. Sensitivity Analysis of collapse scope to explore effect of different micro-parameters such as contact bond normal strength, shear bond normal strength, particle friction coefficient, and stiffness ratio (kn/ks) on shape of single tunnel roof collapse

Figure 12 shows the failure mechanism of the tunnel roof corresponding to density = 2600 kg/m^3, porosity = 0.08, contact young modulus = 1 GPa, vertical distance between tunnel center and footing = 30 m, and confining pressure = 0.01 MPa. According to Figure 12a, it can be concluded that the widths of the collapse zone tend to decrease as the parameter contact bond normal strength increases. Figure 12b shows that the widths of the collapse zone tend to decrease as the parameter contact bond shear strength increases. From Figures 12c and 12d, it is clear that the failure zone is constant by increasing both f the particle friction coefficient and stiffness ratio.

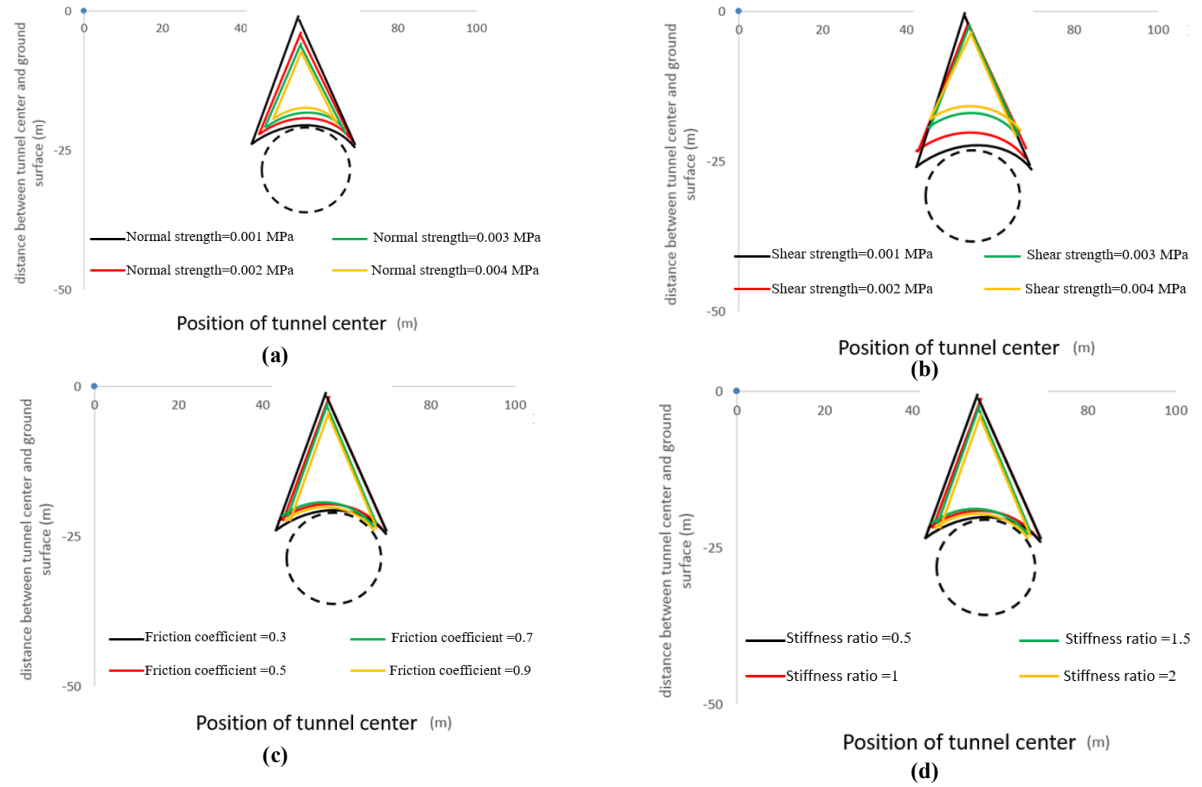

Figure 12. Effects of different parameters on the failure mechanisms of single tunnels: (a) Effects of contact bond normal strength on failure mechanisms, (b) Effects of shear bond normal strength on failure mechanisms, (c) Effects of particle friction coefficient on failure mechanisms, (d) Effects of stiffness ratio (kn/ks) on failure mechanisms.

4. Conclusions

- The volume of the collapsed wedge reduces by augmenting the vertical and horizontal spacing between the tunnel and the foundation.
- The volume of the collapsed zone from the left side of the tunnel decreases by increasing the horizontal spacing between the tunnel and the foundation.
- For each configuration of the horizntal destance between the tunnel and the foundation, the ground settlement was reduced by increasing the vertical spacing between the tunnel center and the foundation. It is to be noted that the ground settlement is decreased by increasing the horizontal destance between the tunnel and the foundation.
- For each configuration of the horizntal destance between the tunnel and the foundation, the vertical displacement of the tunnel roof was decreased by augmenting the vertical spacing between the tunnel center and the foundation. It is to be noted that the vertical displacement of the tunnel roof is decreased by increasing the horizontal distance between the tunnel and the foundation.
- The widths of the collapse zone tend to decrease as the parameter contact bond normal strength increases.
- The widths of the collapse zone tend to decrease as the parameter contact bond shear strength increases.
- The failure zone was constant by increasing both the particle friction coefficient and stiffness ratio.

References

[1]. Lee, GTK., Ng, CWW. (2005). Effects of advancing open face tunneling on an existing loaded pile. J Geotech Geoenviron Eng, Vol. 131(2):193-201.

[2]. Peck, R.B. (1969). Deep excavation and tunneling in soft ground. In: State of the art report, 7th international conference on soil mechanics and foundation engineering, Mexico City, pp. 225-290.

[3]. Cording, E.J. and Hansmire, W.H. (1975). Displacement around soft ground tunnels. In: Proceedings of the Pan-American Conference of Soil Mechanics and Foundation Engineering, Vol. 4: 571-663.

[4]. Attewell, P.B. and Hurrell, M.R. (1985). Settlement development caused by tunneling in soil. Ground Eng. Vol. 18, 17-20.

[5]. Loganathan, N. and Poulos, H.G. (1998). Analytical prediction for tunneling-induced ground movements in clays. J. Geotech. Geoenviron. Eng. Vol. 124(9), 846-856.

[6]. Bobet, A. (2001). Analytical solution for shallow tunnels in saturated ground. J. Eng. Mech., Vol. 127(12), 125-137.

[7]. Rowe, R.K., Lo, K.Y., and Kack G.J. (1983). A method of estimating surface settlement above tunnels constructed in soft ground. Can. Geotech. J., Vol. 20, 11-22.

[8]. Addenbrooke, T.I. (1996). Numerical modelling in Stiff clay. PhD Thesis, Imperial College, London, UK.

[9]. Franzius, J.N., Potts, D.M., and Burland, J.B. (2005). The influence of soil anisotropy and k on ground surface movements resulting from tunnel excavation. Geo-technique, Vol. 55(3), 189-199.

[10]. Zhao, Y. and Zhang, Y. (2019). Fracture behaviors of tunnel lining caused by multi-factors: A case study. Advances in Concrete Construction, an Int'l Journal, Vol. 8(4): 22-33.

[11]. Jain, P. and Chakraborty, T. (2018). Numerical analysis of tunnel in rock with basalt fiber reinforced concrete lining subjected to internal blast load. Geo-mechanics and Engineering, An Int'l Journal, Vol. 4(1):56-76.

[12]. Thai, D. and Nguyen, D. (2021). Safety assessment of an underground tunnel subjected to missile impact using numerical simulations. Computers and Concrete, an Int'l Journal, Vol. 27(1):87-98.

[13]. Zhang, B., Wang, X., Zhang, J.S., and Meng, F. (2017). Three-dimensional limit analysis of seismic stability of tunnel faces with quasi-static method, Geo-mechanics and Engineering, an Int'l Journal, Vol. 13(2):23-34.

[14]. Li, T.Z. and Yang, X.L. (2019). Face stability analysis of rock tunnels under water table using Hoek-Brown failure criterion. Geo-mechanics and Engineering, an Int'l Journal, Vol. 18(3): 53-66.

[15]. Yang, X.J., Deng, F.H., Wu, J.J., and Wang, F.Q. (2009). Response of carrying capacity of piles induced by adjacent metro tunneling. Min Sci Technol, Vol. 19: 176-81.

[16]. Zhang, J., Li, S. (2017) Grouting effects evaluation of water-rich faults and its engineering application in Qingdao Jiaozhou Bay Subsea tunnel, China. Geo-mechanics and Engineering, an Int'l Journal, Vol. 12(1): 98-111.

[17]. Aalianvari, A. (2017). Combination of engineering geological data and numerical modeling results to classify the tunnel route based on the groundwater seepage. Geo-mechanics and Engineering, an Int'l Journal. Vol. 13(4): 67-78.

[18]. Hallaji Dibavar, B. (2019). 3D Numerical Investigation of Ground Settlements Induced by Construction of Istanbul Twin Metro Tunnels with

Special Focus on Tunnel Spacing , periodica plytechnica civil engineering, Vol. 5(1): 1225-1234.

[19]. Yan, q. (2019). 3D Numerical Simulation of Shield Tunnel Subjected to Swelling Effect Considering the Non-linearity of Joint Bending Stiffness, periodica plytechnica civil engineering, Vol. 8(4): 751-762.

20]. Zhao, h. (2016). Reliability-based Support Optimization of Rock-bolt Reinforcement around Tunnels in Rock Masses, periodica plytechnica civil engineering, Vol. 3(1): 250-258.

[21]. Mair, R.J. (1979). Centrifugal modelling of tunnel construction in soft clay. PhD Thesis, Cambridge University, Cambridge, UK.

[22]. Taylor, R.N. (1984). Ground movements associated with tunnels and trenches. PhD Thesis, Cambridge University, Cambridge, UK.

[23]. Cooper, M.L., Chapman, D.N., Rogers, C.D.F., and Chan, A.H.C. (2002). Movements of the Piccadilly line tunnels due to the heath row express construction. Geo-technique, Vol. 52(4), 243-257.

[24]. Suwansawat, S. and Einstein, H.H. (2007). Describing settlement troughs over twin tunnels using a superposition technique. J. Geo-tech. Geo-environ. Eng., Vol. 133(4), 445-468.

[25]. Addenbrooke, T.I. and Potts, D.M. (2001). Twin tunnel interaction surface and subsurface effects. Int. J. Geomech., Vol. 1, 249-271.

[26]. Hunt, D.V.L. (2005). Predicting the ground movements above twin tunnels constructed in London clay. Ph.D. Thesis, University of Birmingham.

[27]. Zhou, L. (2018). The effect of radial cracks on tunnel stability. Geo-mechanics and Engineering, An Int'l Journal, vol. 15(2): 59-67.

[28]. Zou, J. (2017). Influences of seepage force and out-of-plane stress on cavity contracting and tunnel opening". Geo-mechanics and Engineering, an Int'l Journal, Vol. 13(6): 111-121.

[29]. Chen, G. (2019). An improved collapse analysis mechanism for the face stability of shield tunnel in layered soils. Geo-mechanics and Engineering, an Int'l Journal. Vol. 17(1): 99-111.

[30]. Eftekhari, E. (2019). An overview of several techniques employed to overcome squeezing in mechanized tunnel; A case study, Geo-mechanics and Engineering, an Int'l Journal, Vol. 18(2): 87-99.

[31]. Gao, W., (2019). Prediction model of service life for tunnel structures in carbonation environments by genetic programming. Geo-mechanics and Engineering, an Int'l Journal, 18(4): 77-88.

[32]. Sun, Q., Bo J., and Dias D. (2019). Viscous damping effects on the seismic elastic response of tunnels in three sites. Geo-mechanics and Engineering, an Int'l Journal, vol. 18(6):51-63.

[33]. Wu, K. (2019). Mechanical analysis of tunnels supported by yieldable steel ribs in rheological rocks ". Geo-mechanics and Engineering, an Int'l Journal, vol. 19(1):121-132.

[34]. Lee, Y. and Yoo, C. (2006). Behavior of a bored tunnel adjacent to a line of loaded piles.Tunn Underger Space Technol, Vol. 21(3-4): 370.

[35]. Wang, L. (2019) Elastic solutions for shallow tunnels excavated under non-axisymmetric displacement boundary conditions on a vertical surface. Geo-mechanics and Engineering, an Int'l Journal, Vol. 19(3): 187-196.

[36]. Xue, Y. (2019) Stability evaluation for the excavation face of shield tunnel across the Yangtze River by multi-factor analysis .Geomechanics and Engineering, an Int'l Journal , Vol. 19(3): 145-161.

[37]. Chapman, D.N., Ahn, S.K., Hunt, D.V.L., and Chan, A.H.C. (2006). The use of model tests to investigate the ground displacements associated with multiple tunnel construction in soil. Tunn. Undergr. Space Technol., Vol. 21 (3-4), 413.

[38]. Chapman, D.N., Ahn, S.K., and Hunt, D.V.L. (2007). Investigating ground movements caused by the construction of multiple tunnels in soft ground using laboratory model tests. Can. Geo-tech. J., Vol. 44,631-643.

[39]. Divall, S. (2013). Ground movements associated with twin-tunnel construction in clay. PhD Thesis, City University London, UK.

[40]. Yoo, C. and Kim, S.B. (2008). Three dimensional numerical investigation of multi faced tunnelling in water bearing soft ground. Can Geotech J, Vol. 45(10): 1467-86.

[41]. Rabcewicz, L. (1964). The new austrian tunneling method. Part one. Water power November. Part two, December 1964 and part three, January 1965.

[42]. Muller, L. (1978). Removing misconceptions on the new austrian tunneling method. Tunn Tunnel, Vol. 10(8): 29-32.

[43].Vermeer, P.A. and Bonnier, P. (1991). Pile settlement due to tunneling. In proceedings of the 10th European cnference on soil mechanics and foundation engineering, Vol. 2, Florence, Italy, Balkema, Rotterdam, The Netherlands, p. 869-72.

[44]. Chen, L.T., Poulous, H.G., and Loganathan, N. (1999). Pile response caused by tunneling. J Geotech Geoenviron Eng, vol. 125(3):207-15.

[45]. Mroueh, H, Shahrour, I. (2002). Three dimensional finite element analysis of the interaction between tunneling and pile foundations. Int J Numer Anal Meth Geomech, Vol. 26: 217-30.

[46]. Lee, C.J. and Chiang, K.H. (2007). Response of single piles to tunneling induced soil movments in sandy ground. Can Geotech J, Vol. 44: 1224-41.

[47]. Cheng, C.Y., Dasari, G.R., Leung, C.F., Chow, Y.K., and Rosser, H.B. (2007). Finite element analysis of tunnel-soil-pile interaction using displacement controlled model. Tunnell Underger Space Technol, Vol. 22(5): 450-66.

[48]. Yoo, C. (2009). Prformance of multi faced tunneling-a 3D numerical investigation. Tunnell Undergr Space Technol, Vol. 24(5): 562-73.

[49]. Qibin, L. and Ping, C. (2021). Crack coalescence in rock-like specimens with two dissimilar layers and pre-existing double parallel joints under uniaxial compression, International Journal of Rock Mechanics and Mining Sciences, Vol. 139: 39-53.

[50]. Lin, Q., Cao, P., Cao, R. *et al* (2020). Mechanical behavior around double circular openings in a jointed rock mass under uniaxial compression. Archives of Civil and Mechanical Engineering, Vol. 20, 19.

[51]. Itasca Consulting Group Inc, Particle flow code in 2-dimen-sions (PFC2D), Version 3.10.

[52]. Potyondy, D,O. and Cundall, P,A, (2004). A bonded-particle model for rock. Int J Rock Mech Min Sci, Vol. 41(8), (2004) 1329–1364.

[53]. Qibin, L. and Ping, C. (2020). Strength and failure characteristics of jointed rock mass with double circular holes under uniaxial compression: Insights from discrete element method modelling, Theoretical and Applied Fracture Mechanics, Vol. 109: 21-38.

[54]. Qibin, L. and Ping, C. (2021). Mechanical behavior of a jointed rock mass with a circular hole under compression-shear loading: Experimental and numerical studies. Theoretical and Applied Fracture Mechanics, Vol. 114: 51-68.

اندرکنش بین تونل و پی سطحی با استفاده از نرم افزار PFC2D

وهاب سرفرازی[1*]،کاوه عسگری[2] و شادمان محمدی بلبان آباد[1]

۱- بخش مهندسی معدن، دانشگاه صنعتی همدان، همدان، ایران
۲- بخش مهندسی معدن، دانشگاه شهید باهنر کرمان، کرمان، ایران

ارسال ۲۰۲۱/۰۵/۱۷، پذیرش ۲۰۲۱/۰۶/۱۷

* نویسنده مسئول مکاتبات: sarfarazi@hut.ac.ir

چکیده:

در این تحقیق، اندرکنش بین تونل و پی سطحی با استفاده از نرم افزارPFC2D مطالعه شده است. در مرحله اول، نرم افزار PFC با استفاده از داده‌های آزمایش دو محوره کالیبره گردید. برای شبیه سازی آزمایش دو محوره، نمونه بین چهار دیوار محصور گردید. با اعمال فشار محصور کننده توسط دیوارهای جانبی و اعمال بار محوری توسط دیوارهای بالایی و پایینی تست انجام شد. با استفاده از داده‌های تنش انحرافی، دوایر موهر ترسیم شد و خصوصیات برشی مدل تعیین شد. در مرحله دوم، یک مدل عددی با ابعاد ۱۰m×۱۰m حاوی تونل و پی سطحی ساخته شد. تونل در ۱۶ آرایش مختلف نسبت به پی قرار گرفت و بارگذاری با نرخ ۰/۰۱۶ mm/s انجام شد. نتایج نشان دادند که موقعیت تونل حجم آسیب را کنترل می‌کند. جابجایی قائم سقف تونل با افزایش فاصله قائم بین تونل و پی کاهش می‌یابد. همچنین نشست زیر پی با کاهش فاصله بین تونل و پی افزایش می‌یابد.

کلمات کلیدی: تونل، پی، نشست، PFC، ناحیه آسیب.